Materials Innovations

HΣXA Publishers

Optical Materials | Research Article | http://doi.org/10.54738/MI.2021.1103

Effect of Temperature on Structure, Morphology, and Optical Properties of TiO_2 Nanoparticles

Sidra Jamil[1]*, Muhammad Fasehullah[2]

1 Department of Physics, NED University of Engineering and Technology, Karachi, 75270, Pakistan
2 State key laboratory of Power Transmission Equipment & System Security and New Technology, Chongqing University, Chongqing, 400044, China

Check for updates

OPEN ACCESS

Received: 23 August 2021
Accepted: 17 November 2021
Published: 30 November 2021

Citation: Jamil S, Fasehullah M (**2021**) Effect of Temperature on Structure, Morphology, and Optical Properties of TiO_2 Nanoparticles. *Materials Innovations* *1* (1), 21-28.

***Correspondence**: (Sidra Jamil)
sidrajamil@swu.edu.cn

Copyright: © 2021 Jamil S, Fasehullah M. This is an open access article distributed under the terms of the Creative Commons Attribution License, which permits unrestricted use, distribution, and reproduction in any medium, provided the original author and source are credited.

Published By Hexa Publishers

This paper reports synthesis of pure and mixed-phase TiO_2 nanoparticles using a sol-gel technique with titanium isopropoxide as a precursor. The prepared samples were then calcined at different temperatures. Variation in calcination temperature has been analyzed on particle size and crystalline phases, morphology, bandgap, and crystallinity using X-Ray Diffraction (XRD), Scanning Electron Microscope-Energy Dispersive X-Ray Spectroscopy (SEM-EDX), and UV-Vis spectroscopic analysis, respectively. Moreover, XRD data reveal anatase and rutile phases of TiO_2 depending on the calcination temperature. From this, one may observe that the calcination temperature greatly influences the presence of anatase and rutile phases of TiO_2. It can change the phase from the metastable anatase phase to the stable rutile phase. Also, increasing the calcination temperature can increase the particle size as estimated by the Scherrer equation, which was found to be 7 nm to 60 nm with a temperature from 400 °C to 1200 °C. SEM analysis shows the growth of spherical-shaped nanoclusters with irregular morphology, whereas EDX spectroscopic analysis confirms the purity of the samples. It has been observed that increasing the temperature reduces the bandgap through UV-Vis spectroscopic analysis. The photocatalytic degradation of Phenol Red was studied by using synthesized anatase TiO_2 nanoparticles.

Keywords: Titanium dioxide, Nanoparticles, Temperature, Optical properties

INTRODUCTION

Semiconducting materials have been extensively investigated to be used as photocatalysts for light-stimulated degradation of environmental pollutants due to their suitable bandgap energies, mainly for the destruction of toxic and non-biodegradable compounds.[1–3] Among various materials, Titanium dioxide or titania (TiO_2) is an eco-friendly, stable, and low-cost ceramic material that is widely recognized as an excellent model photocatalyst for environmental purification due to its strong oxidizing ability to create photogenerated holes, chemical stability, and non-toxicity.[4–6] TiO_2 usually exists in three crystalline phases, anatase, rutile, and brookite. Anatase and rutile are tetragonal, whereas brookite belongs to the orthorhombic crystalline system. Rutile is a thermodynamically stable phase possessing less photoactivity, enabling it to be used as a pigment and sunscreens[7]. In contrast, the brookite

and anatase phases are metastable while anatase is more photoactive, having a bandgap of 3.2eV.[4,8,9] However, its large bandgap doesn't enable it to absorb light in the visible region. Its photocatalytic efficiencycan be enhanced by tuning the bandgap either by doping with transition metals or by strain.[10] TiO_2 has many applications in the electronic industry, such as MOSFET and gas sensors at high temperatures. It has remarkable usage in the pigment industry due to its high refractive index (typically 3.87 for rutile and 2.5-3 for anatase). TiO_2, when synthesized at the nanoscale, has applications in dye-sensitized solar cells, production and storage of hydrogen, lithium-ion rechargeable batteries, antibacterial and self-cleaning ability.[3,11] The temperature calcination enables the anatase phase of TiO_2 to be transformed into brookite and rutile phases.[12]

The potential of titania is strongly based on its morphology, crystalline structure, and average particle size.[13] The specific surface area is a critical requirement to improve the catalytic activity of TiO_2, which certainly depends on particle size.[14] Several methods have been employed to prepare TiO_2 at the nanoscale[15], such as precipitation[16], microemulsion[17], hydrothermal[18], and sol-gel[19]. Amongst all, sol-gel is the most suitable technique to synthesize nanosized metal oxide materials at low temperatures with high photocatalytic activity, homogeneity, and high purity.[6]

The sol-gel process modifies a liquid into a solid phase, sol to gel[19]. The sol-gel process usually requires the assimilation of metal alkoxides (sol) solution into a three-dimensional polymer matrix (gel). Once the precursor is fully integrated into the matrix, its polymerization is initiated by water, which undergoes a hydrolysis reaction that forms the product upon aging. The final step is the calcination of colloids at different temperatures and durations, which causes the particle agglomeration and usually results in causing polydispersity. Since the reaction is the hydrolysis of metal alkoxides, tailoring various types of nanoparticles is possible, while the overall reaction is simplistic[14,20,21].A.K. Tripathi et al. prepared pure and mixed-phase TiO_2 by sol-gel method calcined at temperature 400 °C to 700 °C having a particle size between 19 nm to 68 nm.[22] Y.-F. Chen et al. obtained anatase powder possessing a diameter of 10nm and a specific surface area of 106.9 m^2/g when calcined at 400 °C and formed a rutile phase at calcination temperatures above 600 °C.[1] H. Lin et al. synthesized nanocrystalline anatase TiO_2 of particle size ranged between 12 to 29 nm by the metal-organic chemical vapor deposition method (MOCVD). It showed that particle size plays a crucial role in changing the bandgap and specific surface area of photocatalysts.[23] Effect of pH was investigated to alter the bandgap of titania nanoparticles by the sol-gel method. The optical analysis reveals the decrease in bandgap with increasing pH.[24] Recently, a hydrothermal synthesis route was adopted to synthesize titania and metal-doped titania nanoparticles. The Ni-doped titania exhibited excellent photocatalytic activity for neutral red and methylene blue dyes.[25] Moreover, the gold-assisted titania Au/TiO_2 hasalso proven to be a photocatalyst for dye degradation as well as photocatalytic hydrogen generation.[26] The present work attempts to demonstrate the effect of calcination temperature on crystalline phases, morphology, and bandgap of TiO_2 nanoparticles via the sol-gel method. To have a clear understanding of the photocatalytic activity of anatase TiO_2, phenol red has been used under UV light for the degradation process.

EXPERIMENTAL SETUP

All reagents, titanium tetra isopropoxide (TTIP), and isopropanol were obtained from Sigma-Aldrich, used without further purification. Deionized water was used as the standard solvent in all experiments.

Synthesis of TiO_2 nanoparticles

TiO_2 nanoparticles were synthesized using the most reliable sol-gel method by hydrolysis of 5 mL solution of Titanium Tetra Isopropoxide (TTIP), an organometallic precursor in a 5 mL solution of isopropanol at room temperature[11]. The mixture was then added at a rate of 5 mL/min. in 200 mL of deionized water resulted in the formation of white colloidal solution and was stirred vigorously for 2 hours. The solution was then covered and aged at room temperature for 24 hours, filtered to get a white paste, and dried at 90 °C for 2 hours to evaporate water and other organic solvents. Figure 1 shows the flowchart of synthesis methodology adopted for the preparation of TiO_2 nanoparticles. To improve crystallization and observe the effect of calcination temperature on prepared samples, the final product was calcined at 400°C to 1200°C for 4 hours in a muffle furnace. The white crystalline powder was ground using ball milling to obtain fine particles of TiO_2.

Characterization of TiO_2 nanoparticles

The XRD analysis of the obtained TiO_2 nanoparticleswas recorded using Bruker D8 Advance X-ray diffractometer (Germany), CuKα (λ = 0.15406 nm) radiation operated at 30 kV and 30 mA at room temperature. Quanta 400 FEG Scanning Electron Microscope (USA) was operated at higher magnification to study the morphology of prepared samples. UV-1800, UV-Vis Spectrophotometer, Shimadzu scientific instruments were used in the range of 300 to 600 nm to study the optical behavior.

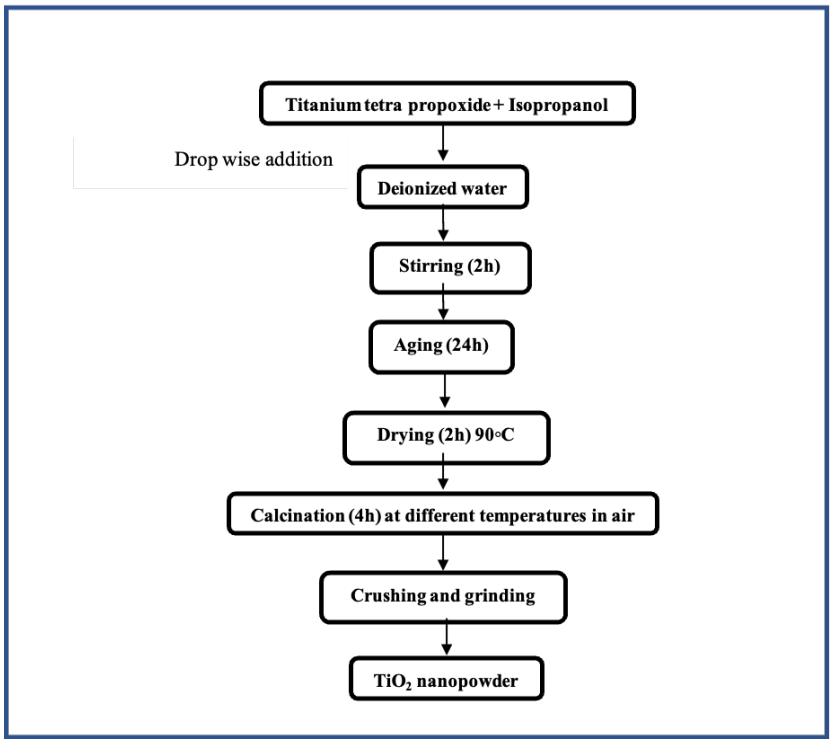

Figure 1. Flow chart for the synthesis of TiO_2 nanoparticles by Sol-Gel route.

RESULTS AND DISCUSSION

X-Ray Diffraction Analysis

The XRD spectra of the obtained TiO_2 nanoparticles are shown in Figure 2 and 3. It can be found that the calcination temperatures greatly affect the occurrence of anatase and rutile phases of TiO_2. At 400 °C and 600 °C, the maximum intensity peak is observed at 2θ = 25.5° for (101) plane, which corresponds to the anatase phase of TiO_2 crystal with tetragonal structure (JCPDS 00-021-1272)[17]. Whereas at 800 °C, 1000°C, and 1200 °C, the XRD peak at $2\theta = 27.7°$ for (110) plane gives evidence of the presence of tetragonal rutile phase of TiO_2 (JCPDS 00-021-1276)[18]. At 600 °C, the less intense peaks of the rutile phase appear, which shows the transformation from anatase to rutile and is said to be the transition state of TiO_2 nanoparticles. The average crystallite size

$$D = \frac{k\lambda}{\beta cos\theta}$$

Where k = 0.89 the shape factor, β is the full-width at half maxima (FWHM) in radians and $2d\sin(\theta) = n\lambda$

The XRD analysis reveals that as temperature increases from 400 °C to 1200 °C, the crystallite size varies from 7 to 60 nm. The lattice parameters ($a = b \neq c$) for tetragonal structure are calculated by;

$$\frac{1}{d^2} = \frac{h^2+k^2}{a^2} + \frac{l^2}{c^2}$$

The XRD parameters, including crystallite size, inter planner spacing, lattice parameter, c/a ratio, and unit cell volume for tetragonal crystalline structure at various temperatures of the strongest peak, have been listed in Table.1

The X-ray density for the samples can be calculated by the relation given below as;

$$\rho = \frac{nM}{NV}$$

Where n = 4 for anatase and n = 2 for rutile, M is the molecular weight, N is the Avogadro's number, and V is the unit cell volume. The bulk density of the naoparticles increases with the increase of calcination temperature from 400 °C to 1200 °C (Table.1).

Broadening of XRD peaks occurs when particle size is less than 100 nm[27,28]. X-ray diffraction peaks show broadening due to strain when the crystallites are small enough. The strain ε can be described by the relation;

$$\varepsilon = \frac{\beta}{4tan\theta}$$

At different calcination temperatures, the strain decreases as the particle size increases. It is already established that with a reduction in particle size, a tremendous increase in the surface area to volume ratio was observed[11]. The higher specific surface area of the anatase phase enables TiO_2 to work efficiently as a photocatalyst[9]. In the present study, the specific surface area was calculated by the relation given below;

$$SSA = \frac{6 \times 10^3}{D \times \rho}$$

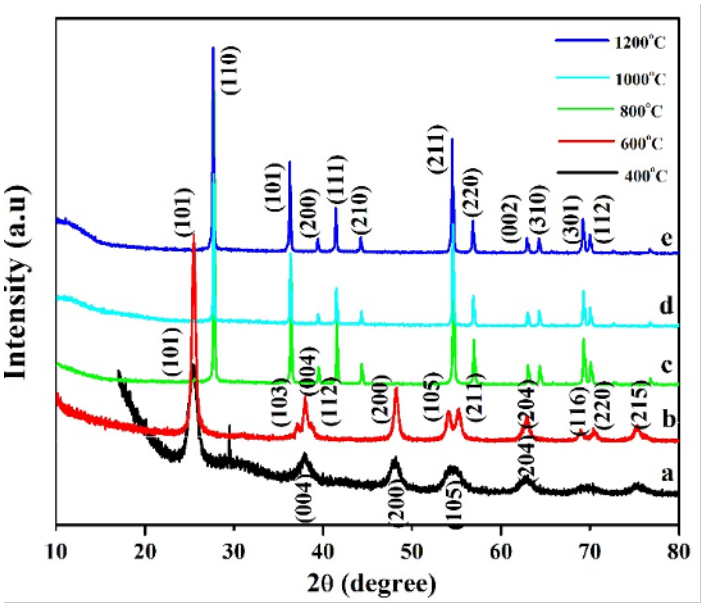

Figure 2. XRD peaks of TiO_2 sample calcinated at temperatures (a) 400 °C, (b) 600 °C , (c) 800 °C , (d) 1000 °C, and (e) 1200 °C.

Table 1. Summary of XRD parameters of TiO_2 nanoparticles at different temperatures

Calculated parameters	**400 °C**	**600 °C**	**800 °C**	**1000 ° C**	**1200 ° C**
2θ (deg)	25.502	25.548	27.778	27.644	27.733
FWHM (radians)	0.019	0.009	0.0028	0.0027	0.0023
Crystallite size D (nm)	7.36	15.12	50.24	52.65	60.52
d-spacing d (Å)	3.49	3.48	3.20	3.22	3.21
(hkl)	101	101	110	110	110
Lattice constant (° A)	a = b = 3.768 c=9.289	a = b = 3.756 c = 9.317	a = b = 4.538 c = 2.964	a=b= 4.56 c= 2.959	a=b= 4.545 c= 2.963
Unit cell volume V = a^2c (Å) ^{3}	131.90	131.46	61.05	61.51	61.21
c/a	2.465	2.48	0.653	0.648	0.652
Strain	1.208	0.587	0.163	0.156	0.135
Surface area to volume ratio (nm^{-1})	0.815	0.396	0.119	0.114	0.099
Bulk density, ρ (gm/cm^3)	4.02	4.03	4.33	4.307	4.32
Specific surface area (m^2 /g)	212.85	103.60	28.16	26.87	23.38
Dislocation density (lines/m^2)	1.85×10^{16}	4.37×10^{15}	3.96×10^{14}	3.61×10^{14}	2.73×10^{14}

Where, D is the crystallite size and r is the density of TiO_2.

The length of dislocation lines per unit volume is defined as dislocation density which is irregularity as well as the defects in the crystalline structure. The larger dislocation density indicates the hardness of the material. Beyond 600 °C, the volume fraction of the anatase phase decreases upon heating, revealing the transformation of phase from anatase to rutile. From the calculation of dislocation densities, one can define the transformation of phase depending on size. As the size increases, the dislocation density decreases. The dislocation density is obtained by using the formula:

$$\delta = \frac{1}{D^2}$$

Stoichiometry and morphology analysis

Energy Dispersive X-ray spectroscopy (EDX) pattern of TiO_2 nanoparticles is

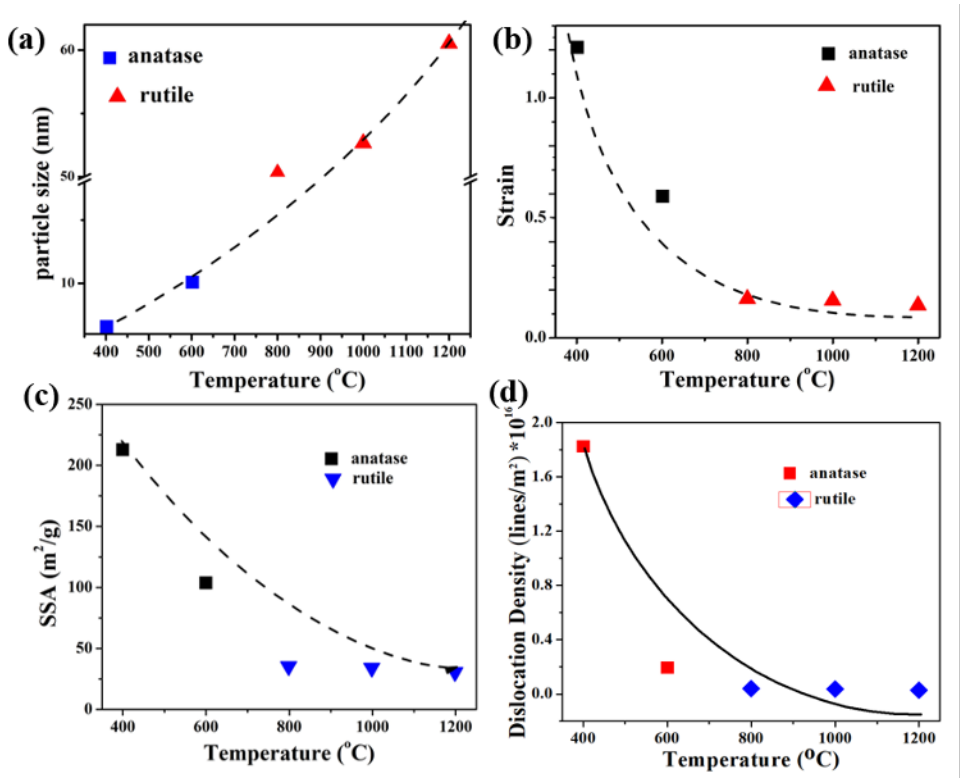

Figure 3. Graph from XRD data illustrates the relation between temperature and (a) particle size, (b) strain, (c) SSA (d) dislocation density.

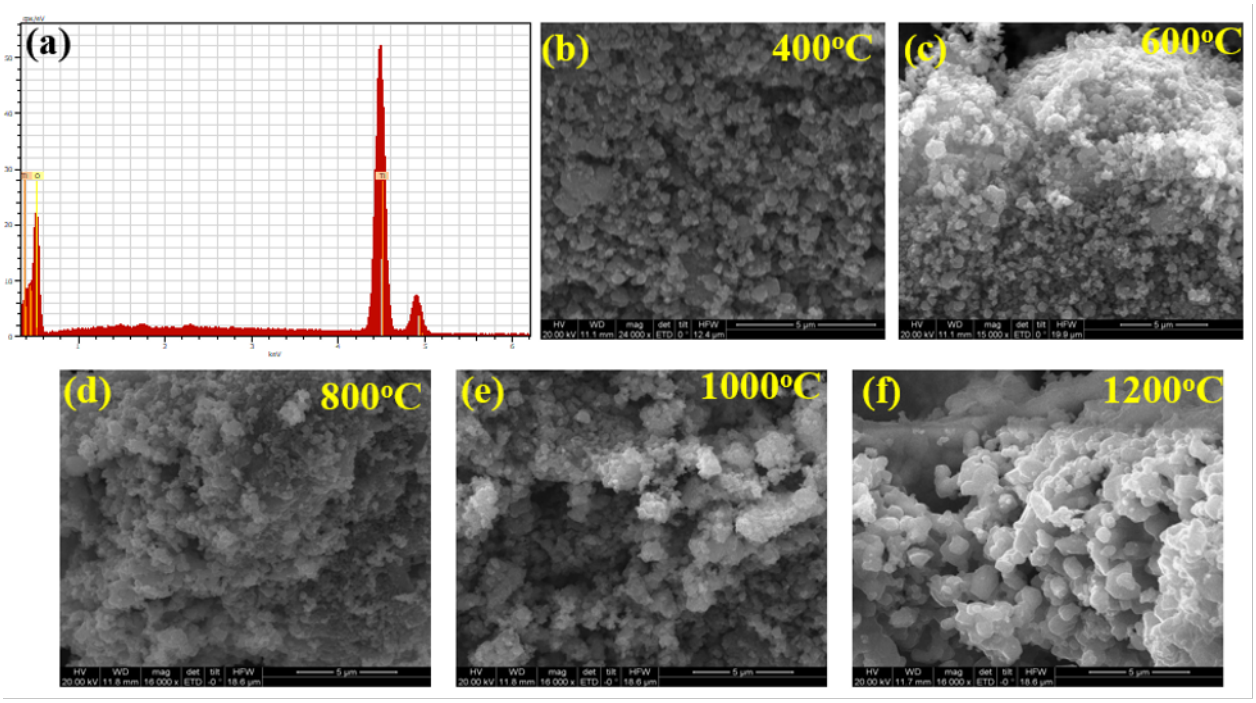

Figure 4. (a) EDX pattern of TiO2 nanoparticles, SEM images of TiO2 samples calcinated at different temperatures (b) 400 °C (c) 600 °C (d) 800 °C (e) 1000 °C, and (f) 1200 °C

Table 2. Energy Dispersive X-Ray (EDX) data of TiO_2 nanoparticles

Sample	Element	Wt %	At %
	Oxygen	38.56	65.26
TiO $_2$	Titanium	61.44	34.74
	Total	100.00	100.00

shown in Figure 4(a), and the chemical composition in wt.% is listed in Table 2. The results validate the high purity of nanoparticles being synthesized.

SEM images of the sample were carried out to estimate the growth and surface morphology of the sample. The grains are spherically shaped with uniform size distribution and irregular distribution in nanoclusters for all temperatures. As the calcination temperature increases, the grain size increases as the particles agglomerate. Figure 4(b-f) shows the SEM images of TiO_2 nanoparticles at different temperatures.

Optical properties

The bandgap energy (E_g) of TiO_2 nanoparticles can be calculated using the following equation;

$$(\alpha h\nu^n) = B(h\nu - E_g)$$

where *h*n is the photon energy, B is a constant, n depends on transition (n= 2/3 for directly forbidden gap, 2 for direct bandgap, and 1/2 for indirect bandgap), and a is the absorption coefficient. The absorption coefficient (a) was determined by Beer-Lambert's relation.

$$\alpha = \frac{2.303A}{d}$$

Where, A is the absorbance from UV-Vis data and d is the path length of the cuvette. At higher calcination temperature, the sample illustrates redshifts due to induced oxygen vacancies which create defects. Absorbance curves of nanoparticles at various calcination temperatures are shown in Figure 5(a). The tauc plot of $(\alpha h\nu)^{1/2}$ versus $(h\nu)$ gives the band gap energy of TiO_2 nanoparticles (Figure 5(b)). The bandgap energy of the sample calcined at 400 °C is found to be 3.44 eV, whereas bulk anatase has a bandgap energy of 3.21 eV and is found to be 2.86 eV calcined as 600 °C, as displayed in Figure 5(c). In nanoscale, as the particle size reduces, the number of overlapping orbitals gets narrower; as a result, the width of the bands decreases. Ultimately, the gap between the valence and conduction bands increases, which increases the bandgap. As temperature increases, the particle size increases, and the bandgap decrease, as reported in literature[29,30]. The bandgap energy of rutile is 2.38 eV, 2.17 eV, and 2.04 eV at 800 °C, 1000 °C, and 1200 °C, respectively. At higher calcination temperatures, the crystallites are larger in size; hence, their optical band gap decreases, supporting photo generation.[31]

Photocatalytic activity of anatase TiO2 synthesized at 400 °C

The photocatalytic activity was carried out in a cylindrical Pyrex-glass beaker with a 1.0 L capacity. A 125-W mercury lamp as an ultra-violet light source was placed just above the beaker, which was filled with 0.6 L of 6 mg/L of Phenol Red solution and 40 mg/L of nanoparticles of TiO_2-400 °C photocatalyst. The whole beaker was cooled with an electric fan from outside the beaker, and the test was carried out at room temperature while fresh air bubbles were introduced into the suspension using a pump. The degradation of model pollutant phenol Red was monitored by taking 5 ml of the suspension at the irradiation time intervals of 1 hour. Each time the suspension was centrifuged to separate the photocatalyst particles from the phenol red solution. Subsequently, the degradation rate was calculated according to the change in absorbance of the dye solution.

The absorption spectra of the samples were recorded by measuring the absorbance at 435 nm corresponding to the maximum absorption wavelength of Phenol red with a UV–Vis absorption spectrophotometer. The concentration of Phenol Red is proportional to the absorbance of Phenol Red according to the Beer-Lambert law, so the degradation efficiency of Phenol Red can be calculated by

$$R = \frac{Co - C}{Co} \times 100\% = \frac{Ao - A}{Ao} \times 100\%$$

Where A_o, A, and C_o, C are the absorbance and concentration of Phenol Red when the reaction time is 0 and t, respectively. Figure 6 shows gradual photo decolorization of the polluted solution; the initial concentration of dye 0.949 decreases to 0.304 after 1 hour of irradiation, which offers 68% degradation, and over one more hour of irradiation, it reduces to 0.249, which results in further degradation of 18%. Hence, TiO_2 sintered at 400 °C possesses an anatase phase with excellent photocatalytic activity.

CONCLUSIONS

Titanium dioxide nanoparticles were successfully prepared using a sol-gel technique with titanium tetraisopropoxide (TTIP) as a precursor. The effect of calcination temperature on the phase transformation of TiO_2 was observed. When the temperature is raised to 700 °C and 800 °C, the anatase phase begins to transform into a rutile phase. The increased calcination temperatures enhance the crystallite size from 7 nm to 60 nm, decreasing the strain and specific surface area to some extent. Tuning of bandgap as a function of calcination temperature was

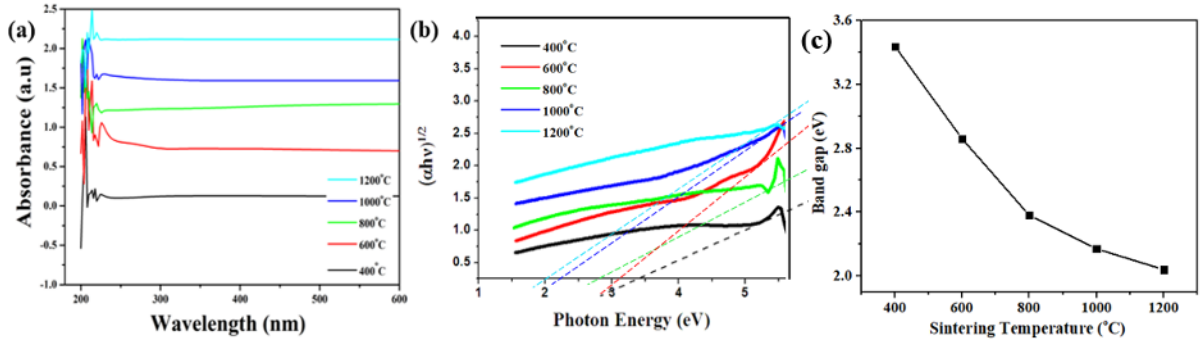

Figure 5. (a) Absorbance curve of TiO_2 nanoparticles at different calcination temperatures, (b) Tauc plots of TiO_2 samples, (c) variation of bandgap with increasing temperature

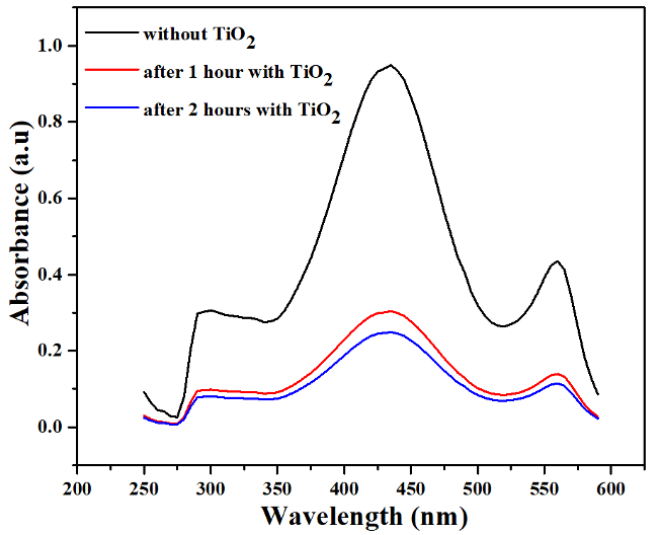

Figure 6. UV-Vis spectra changes of Phenol red (6 mg/L) in aqueous nano TiO_2 dispersion (40 mg/L) irradiated under UV light at a varying time at 0, 1, and 2 hours. Inset shows the normalized absorbance at 435 nm.

observed from tauc plots. The SEM-EDX results showed the purity, chemical composition, and morphology of TiO_2 nanoparticles. The photocatalytic test was carried out, which degraded the model pollutant Phenol Red up to a great extent. In summary, the sintering temperature dramatically influences the phase stability and transformation of titanium dioxide nanoparticles, and an anatase phase acts as an outstanding photocatalyst.

ACKNOWLEDGMENTS

The authors acknowledge NED University of Engineering and Technology for providing a platform to conduct this research work.

References

1) Chen, Y. F.; Lee, C. Y.; Yeng, M. Y.; Chiu, H. T. The effect of calcination temperature on the crystallinity of TiO2 nanopowders. *Journal of Crystal Growth* **2003**, *247* (3), 363–370, DOI: 10.1016/S0022-0248(02)01938-3.
2) Behnajady, M. A.; Eskandarloo, H.; Modirshahla, N. F.; Shokri, M. M. N. F.; Shokri, M. Sol-gel low-temperature synthesis of stable anatase-type TiO2 nanoparticles under different conditions and its photocatalytic activity. *Photochemistry and Photobiology* **2011**, *87* (5), 1751–1097, DOI: 10.1111/j.1751-1097.2011.00954.x.
3) Ahmed, M. A.; El-Katori, E. E.; Gharni, Z. H. Photocatalytic degradation of methylene blue dye using Fe2O3/TiO2 nanoparticles prepared by sol-gel method. *Journal of Alloys and Compounds* **2013**, *553*, 19–29, DOI: 10.1016/j.jallcom.2012.10.038, available at https://doi.org/10.1016/j.jallcom.2012.10.038.
4) Khataee, A.; Mansoori, G. A. Nanostructured Titanium Dioxide Materials. Nanostructured Titanium Dioxide Materials. 2011.
5) Panpan, Z.; Bing, T.; Wen, X.; Fei, W.; Xiaoyi, W.; Jiaqing, X.; Jihua, L. Preparation and Characterizations of TiO2 Nanoparticles by Sol-Gel Process using DMAC Solvent. *Proceedings of the 2015 2nd International Conference on Machinery, Materials Engineering* **2015**, 892–895.
6) Elsellami, L.; Dappozze, F.; Fessi, N.; Houas, A.; Guillard, C. Highly photocatalytic activity of nanocrystalline TiO2 (anatase, rutile) powders prepared from TiCl4 by sol-gel method in aqueous solutions. *Process Safety and Environmental Protection* **2018**, *113*, 109–121, DOI: 10.1016/j.psep.2017.09.006, available at

https://doi.org/10.1016/j.psep.2017.09.006.
7) Sharon, M.; Modi, F.; Sharon, M. Titania based nanocomposites as a photocatalyst: A review. *AIMS Materials Science* **2016**, *3* (3), 1236–1254, DOI: 10.3934/matersci.2016.3.1236.
8) Azizi, K. F.; Bagheri-Mohagheghi, M. M. Transition from anatase to rutile phase in titanium dioxide (TiO2) nanoparticles synthesized by complexing sol-gel process: effect of kind of complexing agent and calcinating temperature. *Journal of Sol-Gel Science and Technology* **2013**, *65* (3), 329–335, DOI: 10.1007/s10971-012-2940-2.
9) Valencia, S.; Marín, J. M.; Restrepo, G. Study of the Bandgap of Synthesized Titanium Dioxide Nanoparticules Using the Sol-Gel Method and a Hydrothermal Treatment. *Applied Physical Chemistry Processes* **2009**, *4*, 9–14, DOI: 10.2174/1874088X01004010009.
10) Yin, W. J.; Chen, S.; Yang, J. H.; Gong, X. G.; Yan, Y.; Wei, S. H. Effective Band Gap Narrowing of Anatase TiO2 by Strain Along a Soft Crystal Direction. *Applied Physics Letters* **2010**, *96*, 221901, DOI: 10.1063/1.3430005, available at https://doi.org/10.1063/1.3430005.
11) Sampreeth, T.; Al-Maghrabi, M. A.; Bahuleyan, B. K.; Ramesan, M. T. Synthesis, characterization, thermal properties, conductivity and sensor application study of polyaniline/cerium-doped titanium dioxide nanocomposites. *Journal of Materials Science* **2018**, *53* (1), 591–603, DOI: 10.1007/s10853-017-1505-8.
12) Zareen, A.; Ali, S.; Irfan, M. The effect of Annealing temperatures on phase and optical properties of TiO2 nanoparticles for solar cell applications. *European Scientific Journal* **2014**, (10), 10–10.
13) Chaudhary, V.; Srivastava, A. K.; Kumar, J. On the Sol-gel Synthesis and Characterization of Titanium Oxide Nanoparticles. *MRS Online Proceedings Library* **2011**, *1352* (1), 1024–1024.
14) Lin, H.; Huang, C. P.; Li, W.; Ni, C.; Shah, S. I.; Tseng, Y. H. Size dependency of nanocrystalline TiO2 on its optical property and photocatalytic reactivity exemplified by 2-chlorophenol. *Applied Catalysis B: Environmental* **2006**, *68* (1), 1–11, DOI: 10.1016/j.apcatb.2006.07.018, available at https://doi.org/10.1016/j.apcatb.2006.07.018.
15) Su, C.; Hong, B. Y.; Tseng, C. M. Sol-gel preparation and photocatalysis of titanium dioxide. *Catalysis Today* **2004**, *96* (3), 119–126, DOI: 10.1016/j.cattod.2004.06.132, available at https://doi.org/10.1016/j.cattod.2004.06.132.
16) Scolan, E.; Sanchez, C. Synthesis and Characterization of Surface-Protected Nanocrystalline Titania Particles. *Chemistry of Materials* **1998**, *10* (10), 3217–3223, DOI: 10.1021/cm980322q, available at https://doi.org/10.1021/cm980322q.
17) Lal, M.; Chhabra, V.; Ayyub, P.; Maitra, A. Preparation and characterization of ultrafine TiO2 particles in reverse micelles by hydrolysis of titanium di-ethylhexyl sulfosuccinate. *Journal of Materials Research* **1998**, *13* (5), 1249–1254, DOI: doi:10.1557/JMR.1998.0178.
18) Wu, M.; Lin, G.; Chen, D.; Wang, G.; He, D.; Feng, S.; Xu, R. Sol-Hydrothermal Synthesis and Hydrothermally Structural Evolution of Nanocrystal Titanium Dioxide. *Chemistry of Materials* **2002**, *14* (5), 1974–1980, DOI: 10.1021/cm0102739, available at https://doi.org/10.1021/cm0102739.
19) Yu, K.; Zhao, J.; Guo, Y.; Ding, X.; Hari, B.; Liu, Y.; Wang, Z. Sol-gel synthesis and hydrothermal processing of anatase nanocrystals from titanium n-butoxide. *Materials Letters* **2005**, *59* (19), 2515–2518, DOI: 10.1016/j.matlet.2005.03.047, available at https://doi.org/10.1016/j.matlet.2005.03.047.
20) Kelly, A., Ed. *Advances in Material Science and Engineering*; Ed. Pergamon: Oxford, 1994.
21) Priyanka, K. P.; Joseph, S.; Thankachan, S.; Mohammed, M. E.; Varghese, T. Dielectric Properties and A.C. Conductivity of Nanocrystalline Titania. *Journal of Basic and Applied Physics* **2013**, *2* (1), 4–7.
22) Bessekhouad, Y.; Robert, D.; Weber, J. V. Preparation of TiO2 nanoparticles by Sol-Gel route. *International Journal of Photoenergy* **2003**, *5*, 496128–496128, DOI: 10.1155/S1110662X03000278.
23) Nagaveni, K.; Sivalingam, G.; Hegde, M. S.; Madras, G. Photocatalytic Degradation of Organic Compounds over Combustion-Synthesized Nano-TiO2. *Environmental Science & Technology* **2004**, *38* (5), 1600–1604, DOI: 10.1021/es034696i.
24) Imran, M.; Riaz, S.; Naseem, S. Synthesis and Characterization of Titania Nanoparticles by Sol-gel Technique. *Materials Today: Proceedings* **2015**, *2*, 5455–5461, DOI: 10.1016/j.matpr.2015.11.069.
25) Sadia, M.; Naz, R.; Khan, J.; Zahoor, M.; Ullah, R.; Khan, R.; Naz, S.; Almoallim, H. S.; Alharbi, S. A. Metal doped titania nanoparticles as efficient photocatalyst for dyes degradation. *Journal of King Saud University - Science* **2021**, *33* (2), 101312.
26) Anderson, J. A. Metal-promoted titania photocatalysis for destruction of nitrates and organics from aqueous environments. *Philosophical Transactions of the Royal Society A: Mathematical, Physical and Engineering Sciences* **2018**, 376–376, DOI: 10.1098/rsta.2017.0060, available at https://doi.org/10.1098/rsta.2017.0060.
27) Theivasanthi, T.; Alagar, M. Titanium dioxide (TiO2) Nanoparticles XRD Analyses: An Insight. *arXiv preprint arXiv:1307.1091* **2013**, DOI: 10.48550/arXiv.1307.1091, available at https://doi.org/10.48550/arXiv.1307.1091.
28) Purushotham, E.; Krishna, N. G. X-ray determination of crystallite size and effect of lattice strain on Debye-Waller factors of platinum nano powders. *Bulletin of Materials Science* **2013**, *36* (6), 973–976, DOI: 10.1007/s12034-013-0553-1.
29) Singh, M.; Singhal, A. In Modeling of Shape and Size Effects for the Band Gap of Semiconductor Nanoparticles. *2nd International Conference on Micro-Electronics and Telecommunication Engineering (ICMETE)* **2018**, 339–342, DOI: 10.1109/ICMETE.2018.00080.
30) Deotale, A. J.; Nandedkar, R. V. Correlation between Particle Size, Strain and Band Gap of Iron Oxide Nanoparticles. *Materials Today: Proceedings* **2016**, *3* (6), 2069–2076, DOI: 10.1016/j.matpr.2016.04.110, available at https://doi.org/10.1016/j.matpr.2016.04.110.
31) Noorimotlagh, Z.; Kazeminezhad, I.; Jaafarzadeh, N.; Ahmadi, M.; Ramezani, Z.; Martinez, S. S. The visible-light photodegradation of nonylphenol in the presence of carbon-doped TiO2 with rutile/anatase ratio coated on GAC: Effect of parameters and degradation mechanism. *Journal of Hazardous Materials* **2018**, *350*, 108–120, DOI: 10.1016/j.jhazmat.2018.02.022, available at https://doi.org/10.1016/j.jhazmat.2018.02.022.